ACS APPLIED MATERIALS & INTERFACES

Research Article

www.acsami.org

Photopolymeric Multifunctional Dendrimer toward Holographic Applications

Yong-Cheol Jeong, Bokyung Jung, and Jung-Ki Park*

Department of Chemical and Biomolecular Engineering, KAIST, 291 Daehak-ro, Yuseong-gu, Daejeon 305-701, South Korea

ABSTRACT: We present a photopolymeric multifunctional dendrimer for holographic applications. In this study, we described a synthesis of multiphotoreactive dendrimer and phase compatible polymer matrix as well as a numerical simulation of the dendrimer. This holographic photopolymer containing a nanosized photoreactive organic dendrimer could address the aggregation issue of conventional inorganic nanoparticle additives and allowed writing-induced shrinkage to be successfully reduced to the extent of acceptable values for 130 μm thick film. In this report, holographic performance including diffraction efficiency (DE), transmission, photosensitivity, modulation of refractive index, polarization sensitivity, and volume shrinkage has been discussed. The page-wise recording by using an amplitude spatial light modulator (SLM) was also demonstrated.

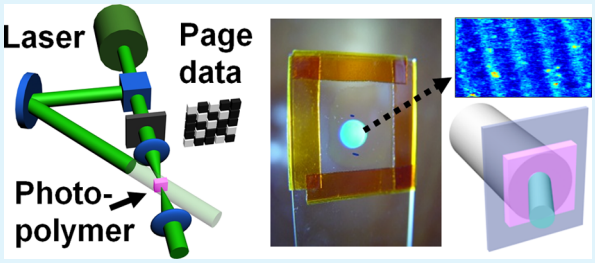

KEYWORDS: *interference pattern, diffraction grating, dendrimer, photopolymer*

INTRODUCTION

In recent decades photopolymers have been extensively studied as holographic recordable media because volumetric holographic optical element can manipulate the incident light at a specific angle (Bragg diffraction).[1] The photopolymers also facilitate fabrication of thick volume gratings via transfer of a light interference pattern without a photomask.[2,3] Furthermore, photopolymers have the advantages of a relatively high refractive index modulation, moderate photosensitivity, and a high dynamic range.[4,5] However, despite these merits of photopolymers, volume shrinkage during photoreaction is an inevitable and critical problem that leads to deterioration of diffraction gratings and significantly decreases the diffraction efficiency (DE) at its Bragg recording angle.[6] Generally, photoreaction causes polymerization of monomers triggered by activated radicals and induces extinction of the microscopic volume in the photopolymers, and thereby, the thickness of photopolymer film is reduced. To address the volume shrinkage issue, intensive research has been done including sol−gel systems,[7−10] cationic ring-opening polymerization systems,[11,12] cross-linked matrix systems,[13,14] and organic−inorganic hybrid systems.[15−20] Among those systems, the organic−inorganic hybrid strategy would be beneficial to enhance mechanical strength of conventional photopolymers by simply incorporating the inorganic nanoparticle additives. Meanwhile, the inorganic nanoparticle-incorporated photopolymer system has an issue of dispersion due to its insolubility in the polymer matrix, which limits the achievable thickness of photopolymer. Since thick photopolymer is important for recording the multiple holograms in the same volume, there has been an effort to enhance the dispersion of inorganic nanoparticle by coating organic materials on the surface of nanoparticle.[21] Within this context, in this study, we presented the organic dendrimer-incorporated photopolymer system as another approach.

EXPERIMENTAL SECTION

Multifunctional Dendrimer and Its Molecular Dynamics Simulation. As mentioned, we introduced a fully soluble organic dendrimer (H30, Boltorn, third generation, 32-terminal hydroxyl groups, M_w = 3500 g/mol, Figure 1a) to address the scattering issue. The dendrimer is an organic molecule that is dissolved within a photopolymer solution at the molecular level. In addition, the relatively high density of the end groups provided by the nature of a fractal-like structure is readily controlled by changing the degree of generation of the dendrimer. This also presents a very simple way of controlling the density of the photoreactive moiety when the end groups are substituted with radical-reactive ones. Although hyperbranched polymer nanoparticles or dendronized macromers were previously introduced for holographic 3D storage, they were nonreactive or only functionalized to have a single reactive end group for each dendrimer rather than multireactive dendrimers.[22,23] To estimate the molecular radius of a dendrimer and the end-to-end trajectory distance between chain ends, we conducted a simulation of the molecular dynamics of H30 by minimizing the conformational energy with the commercial software Materials Studio. It revealed that a size of chemical moiety of less than 0.7 nm in radius could pass through the chains of H30 (Figure 1b), confirming that monomers diffuse without sacrificing the diffusivity, which is not the case with conventional nanoparticles acting like obstacles.[24]

Holographic Recording of Dendrimer-Incorporated Photopolymer. To investigate the effect of photoreactive dendrimers on holographic performance according to reactive groups, we prepared two types of dendrimers functionalized with different lengths of linkage, which are denoted as H30-MA (methacrylate) and H30-UA

Received: July 5, 2012
Accepted: September 5, 2012
Published: September 5, 2012

   dx.doi.org/10.1021/am3012406 | ACS Appl. Mater. Interfaces 2012, 4, 4921−4926

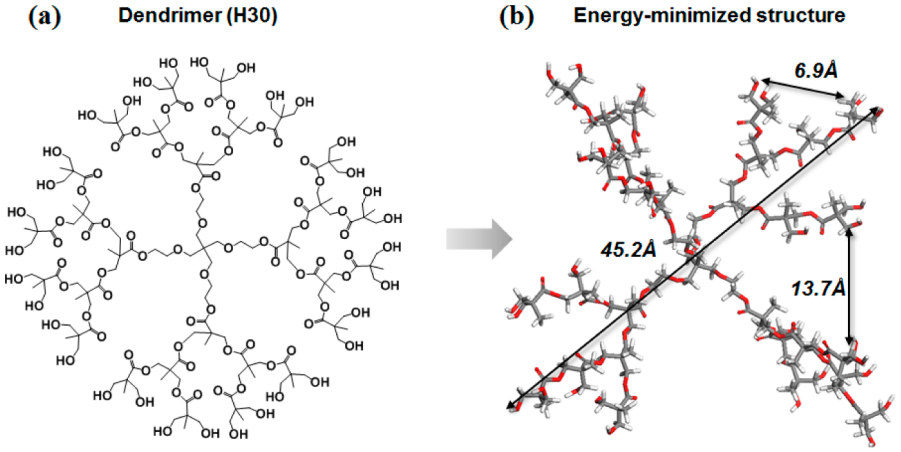

Figure 1. (a) Chemical structure of dendrimer, H30. (b) The geometrically energy-minimized conformational structure of the dendrimer gives an end-to-end distance of 4.5 nm and the shortest distance between the end groups is 0.7 nm.

(10-undecenoyl group), respectively. To modify H30 to have a photoreactive function, hydroxyl terminal groups of H30 were substituted with acryloyl chloride group, a radical sensitive unit, via Fischer esterification reaction, as represented in Figure 2a.[25] The

(b)

	Name	Structure	Description
Matrix	Poly(MMA-co-MAA)	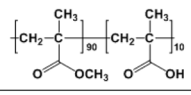	Copolymer matrix
Photosensitive materials	AA	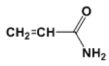	Monomer
	DMAcA	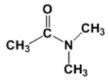	Plasticizer Compatibilizer
	I784	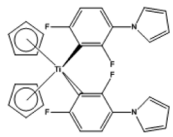	Initiator (radical generator)
	H30	H30-MA, H30-UA	Photoreactive dendrimer

Figure 2. (a) Synthetic scheme for preparation of the photoreactive dendrimers. (b) Chemical structures of materials of photopolymer.

matrix polymer for transparent and phase compatible photopolymers was also synthesized by copolymerization of 90 mol % of methyl methacrylate and 10 mol % of methacrylic acid as monomers using azobisisobutyronitrile (AIBN) as a radical initiator. The detailed procedure was explained in the previous reports.[26,27]

For the preparation of photopolymers, the matrix polymer/monomer (acrylamide, AA)/plasticizer (dimethylacetami-de)/initiator (Irgacure784) was formulated at the ratio 46:16:37.5:0.25 wt %, while 0.6 wt % of dendrimers was added. All the chemical structures of used materials are listed in the Figure 2b. The photopolymer materials were dissolved by the solvent tetrahydrofuran. The photopolymer solution was cast on the glass substrate and dried in the dark for 24 h, resulting in a transparent and flat film of 130 μm. The theoretical refractive index of the mixed photopolymer system was computed by Lorentz–Lorenz equation,[28] defined as eq 1:

$$\frac{n^2-1}{n^2+2}=\sum_m \Phi_m \frac{n_m^2-1}{n_m^2+2} \quad (1)$$

where n, n_m, and Φ_m are refractive index of photopolymer, refractive index, and volume fraction of each component, respectively. The theoretical refractive index of film was calculated to be 1.466, which will be used to evaluate the modulation of refractive index later in the Discussion section.

To study the modulation of the refractive index of the photopolymer, we traced the DE behavior as a function of the exposure dose of light interference by two-beam coupling, as shown in Figure 3a. A diode-pumped solid-state microchip laser (Melles Griot, λ = 532 nm, power = 20 mW, beam diameter = 1.1 mm) was spatially filtered and expanded to 5 times. The beam was split into two mutually coherent writing beams with an intensity ratio of 1:1 and at an external angle (θ) of 15.4° to the normal (i.e., the angle between the beam bisector and the surface normal). The final laser intensity was attenuated to be 4.5 mW/cm^2. To elucidate the grating period precisely, we measured grating spacing with atomic force microscopy (AFM), which was revealed as 1.06 μm, as shown in Figure 3b. It correlates well with the calculated grating period ($\Lambda = \lambda/(2 \sin \theta)$) of the photopolymer film as we expected to be set. Finally, it gives spatial frequency of 998 lines/mm.

The DE was evaluated in real time by monitoring the intensity of diffracted beam with photodiode (Ophir, PD300-SH) and homemade Labview program, where DE and transmission were defined as eqs 2 and 3, respectively.

$$\mathrm{DE}=\frac{\text{1st diffraction}}{\text{input}}=\frac{I_d}{I_i} \quad (2)$$

$$\text{transmission}=\frac{\text{output}}{\text{input}}=\frac{I_d+I_t}{I_i} \quad (3)$$

Detailed experimental information of holographic exposure for volume grating formation is schematically illustrated in Figure 3.

RESULTS AND DISCUSSION

Optical Properties of DE, Scattering Loss, and Photosensitivity. Without dendrimers, as shown in Table 1, 49.6% of the DE was obtained where the refractive index modulation was 1.54 × 10^{-3} as calculated by Kogelnik's coupled wave theory,[29] which seems to be relatively low compared to conventional photopolymers (note that the internal angle of 10.5°, calculated by the Snell's law with the external angle and the theoretical refractive index of photopolymer, was used for evaluating the modulation of refractive index). By including the photoreactive dendrimer having

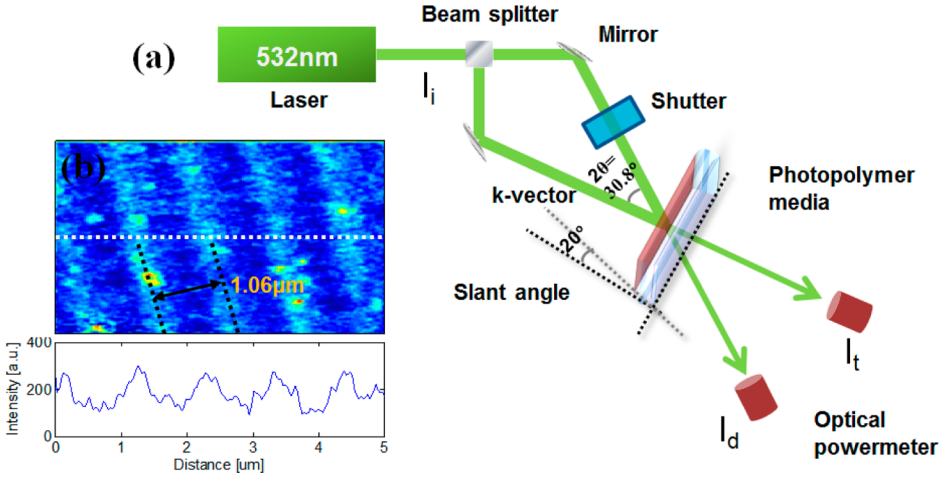

Figure 3. (a) Schematic illustration of holographic recording by using a two-beam coupling. (b) AFM image of holographically recorded photopolymer surface and its corresponding intensity profile.

Table 1. Optical Properties of Photopolymers

material	DE [%]	TE [%]	Δn [10^{-3}]	S [10^{-5} cm^2/mJ]
AA	49.6	94.2	1.54	2.91
AA_H30-MA	72.6	93.7	1.95	4.75
AA_H30-UA	79.0	94.1	2.15	5.29

different end groups, H30-MA and H30-UA, the DE increased to 72% and 79%, respectively, with steeper initial growing slope compared to a no-dendrimer system, as shown in Figure 4a. Furthermore, the transmittance of dendrimer-included photopolymers was 93.7 and 94.1% in the case of H30-MA and H30-UA, respectively, which is similar to 94.2% of photopolymer without dendrimer. Considering 5−6% loss in transmission of glass substrate and film by both reflection and absorption, it is clear that the scattering loss was controlled well. Meanwhile, the grating build-up was accelerated by the high photoreaction rate due to the more concentrated reactive groups of dendrimers, as the photosensitivity is shown in Figure 4b. Thus, the monomer diffusion is triggered by the concentration gradient of monomers, boosting growth of the grating at an early stage. It is interesting that a higher refractive index modulation was obtained with H30-UA at an earlier exposure time whereas the reduction in the DE at the plateau region was relatively severe compared with H30-MA. This can be explained by the combined effect from the reactivity of the dendrimer end groups and the grating strength of the photopolymer system.[30] In general, it is known that the double bond of methacrylate is much more reactive than that of the undecenoyl group because the carbonyl group of methacrylate side chain (H30-MA) is electron-withdrawing whereas the alkyl side chain (H30-UA) is an electron-donating group. Meanwhile, the mobility of functional end groups influences the reactivity when those are bound to the surface of nanoparticle or dendrimer. In this study, it was found that the photopolymerization was dominantly affected by the chain mobility from the flexible and long alkyl linkage rather than the chemical reactivity of double bond itself. However, the DE decreased gradually with additional holographic exposure, which could be interpreted by the following reasons: (1) counter-diffusion of photopolymerized chains because of the polymer concentration gradient across the gratings and (2) blurred edge of grating by phase-separated polymer chains when the photopolymerized polymer is not compatible to the matrix polymer.[26,30,31]

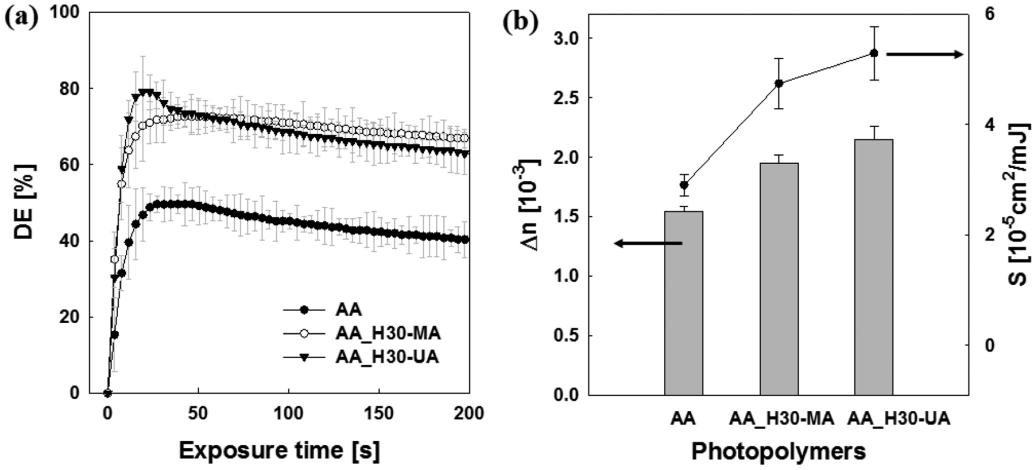

Figure 4. (a) Traces of diffraction behavior in real time with respect to inclusion of functionalized dendrimer. (b) Modulation of refractive index, evaluated from Kogelnik theory on volume grating, and photosensitivity defined as $\Delta n/E_{80}$, where E_{80} is required energy to reach 80% of the maximum DE.

dx.doi.org/10.1021/am3012406 | ACS Appl. Mater. Interfaces 2012, 4, 4921−4926

Considering the decrease in DE without significant scattering loss, we inferred that the DE was reduced by deterioration of sinusoidal modulation of refractive index attributed to the counter-diffused photopolymerized polymers.

We also evaluated the polarization sensitivity of the volume gratings in terms of diffraction efficiency by arranging and rotating a halfwave plate in between the recorded photopolymer film and the linearly polarized laser. Figure 5 shows the response of diffracted beams at the first order for the red-visible laser (wavelength of 633 nm) as a function of the rotation angle of the halfwave plate. The diffraction efficiency varied from 100 to 80% as the polarization of incident light changed as expected.

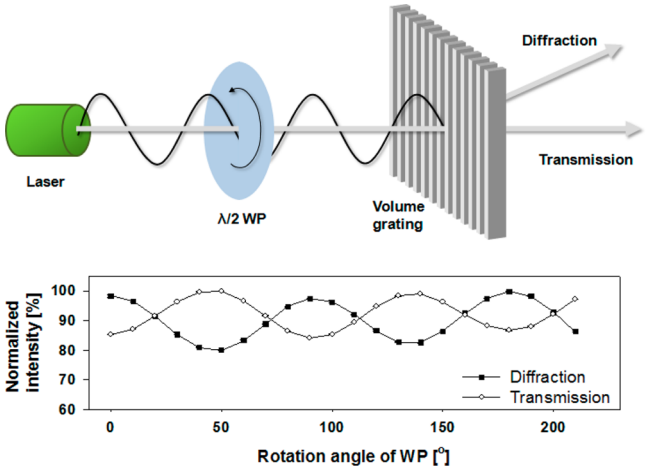

Figure 5. Schematic illustration of the experiment of measuring the diffracted and transmitted light intensity as a function of polarization angle of incident light.

Volume Shrinkage and Multiplexing. To study the dendrimer effect on grating distortion, volume shrinkage was also investigated by measuring the deviation angle from the Bragg angle by rotating the photopolymer samples with a resolution of 0.05° after completion of holographic exposure (note that the gratings were recorded at an asymmetric external angle of 20°). It revealed that the deviation angle to the Bragg recording angle was 0.20° and 0.25° in case of H30-MA and H30-UA, respectively, which is less than two times of a photopolymer without any H30, which reflects how photoreactive dendrimers improved the mechanical strength of the gratings represented in Figure 6a. The evaluated volume shrinkage coefficients (VS_B), defined as $(1 - \tan(\theta)/\tan(\theta + \Delta\theta))$ where θ and $\Delta\theta$ are the asymmetric internal angle and the Bragg angle detuning, respectively, are shown in Figure 6b.

We also measured the dimensional change in the volume by measuring the density change of the photopolymers using an electronic densimeter (SD-120 L, Mirage Co., with an accuracy of 0.0001 g/cm^3), which shows the total shrinkage in volume at all directions rather than only at the vertical direction. Our measurements disclosed that the volume shrinkage decreased from 3.2% to 1.56% and 1.41% upon introducing H30-MA and H30-UA, respectively, where these values were slightly higher than those evaluated from deviated angles. The reduction in dimensional change during photoreaction could be explained in terms of the reinforced mechanical strength of the grating induced by an in situ reaction between AA monomers and multiarmed dendrimers. This polymerization prevents entanglement of polyacrylamide and provides additional mechanical strength, which is expected to reduce the volume change in the

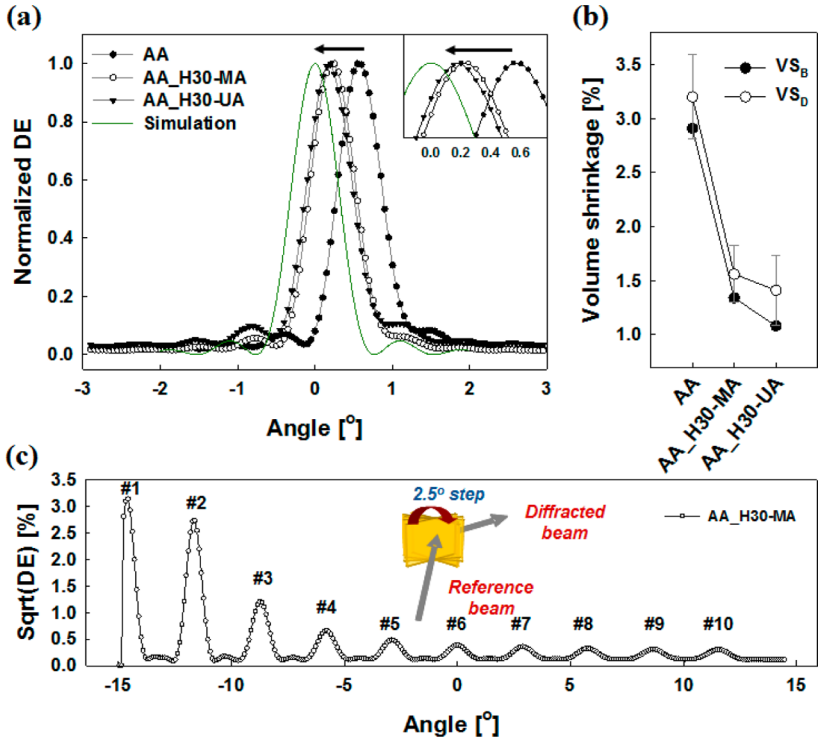

Figure 6. (a) Angular selectivity of photopolymers, which denotes less Bragg angle deviation in the case of H30-MA and H30-UA compared with the case of no H30 photopolymer. (b) Coefficients of volume shrinkage calculated by Bragg angle deviation (VS_B) and change in density (VS_D) during holographic reaction. (c) Multiplexing of 10 different holograms with an interval degree of 2.5° at the same volume. The number indicates the recorded order of the holograms.

dx.doi.org/10.1021/am3012406 | ACS Appl. Mater. Interfaces 2012, 4, 4921−4926

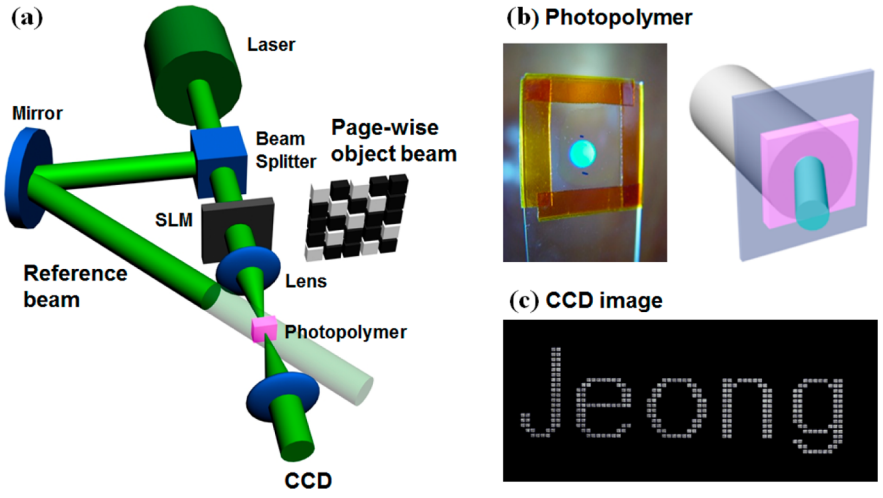

Figure 7. (a) Schematic illustration of holographic page-wise digital recording with SLM. (b) Digital camera picture of diffraction beam when white light was illuminated to holographically recorded spot of H30-MA (left) and its schematic illustration (right). (c) CCD captured image of retrieval data with plain reference beam.

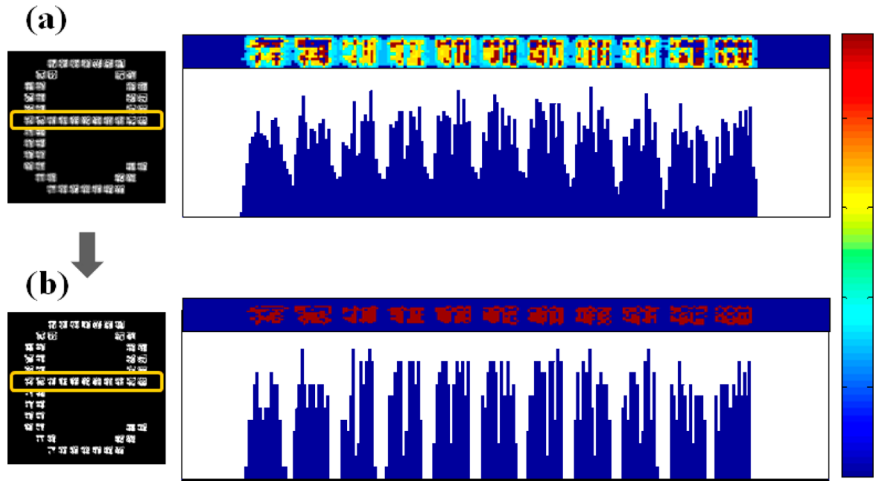

Figure 8. Signal intensity profile of 11 pixels in the retrieved page-data denoted as yellow box and its color-mapped image, where red color indicates high value. (a) Raw CCD image in gray scale; "on" pixels were not separated from each other. (b) Binary-converted image with proper threshold; all pixels were recognized without crosstalk.

photopolymers. Furthermore, 10 different multiple holograms were recorded at the same volume of photopolymer by rotating the recording medium at an interval of 2.5°, which is two times higher than the full width half-maximum (fwhm) of angular selectivity and enabled us to achieve multiplexing of the gratings without a crosstalk problem, as shown in Figure 6c.

Page-wise Recording and Image Analysis. To demonstrate the feasibility of holographic data storage as a practical application, page-wise digital data was holographically recorded and retrieved using an amplitude SLM with a resolution of 75 × 62 (4650 bits/page). The object beam was encoded by passing it through the SLM and then converged at the photopolymer film with the coupling of the reference beam, as illustrated in Figure 7a. After completion of the holographic recording, the photopolymer film was kept in the dark for 20 min until the active radicals were totally consumed, followed by UV postfixing for 10 min. As shown in Figure 7b, when the white light was illuminated to the recorded photopolymer, it was observed that blue-visible light was diffracted at a certain viewing angle, as shown in the picture. In addition, by illuminating the reference beam to the recorded spot of medium at its Bragg angle, quite well-defined pixel data were captured with a charge-coupled camera (CCD), shown at the bottom of Figure 7c, revealing high quality optical film. Generally, surface flatness is one of the most critical factors that influence image quality in transparent amorphous polymer film, which is determined by the evaporation rate of the solvent. Since solvent evaporation that is too rapid results in wrinkling on the surface of the photopolymer, a drop-casted photopolymer solution was kept in a confined case that provided sufficient time for the flat surface to form. We expect this to become an essential procedure for a system based on a linear polymer matrix requiring solvent evaporation without cover glass.

To verify the fidelity of page-wise recording, the retrieved CCD images (256 gray) were analyzed by using a homemade Matlab code. Figure 8a represents the signal intensity profile of page-data pixels, where the retrieved data was used without any postprocessing. It shows that on/off page information was clearly retrieved as individual white and black pixels with good signal-to-noise ratio (SNR), reflecting a negligible degree of scattering. However, as shown in the magnified and color-

dx.doi.org/10.1021/am3012406 | ACS Appl. Mater. Interfaces 2012, 4, 4921−4926

mapped image on the graph, it seems that boundaries of the adjacent white pixels are much blurred, leading to deteriorated accuracy of reading. Although it could be solved by reducing the incoming light intensity by faster shutter speed of CCD, the effective intensity of the signal is also sacrificed. To address the aforementioned problem, we converted the gray scale image of raw data to binary-scale to exclude artifact with proper threshold, as shown in Figure 8b. After processing the image of CCD captured data, all white pixels were clearly recognized without a crosstalk problem.

CONCLUSIONS

In conclusion, we described a photoreactive dendrimers-included photopolymer, which was designed to enhance modulation of the refractive index as well as the growing speed with controlled volume shrinkage without a light scattering problem. Photopolymers containing multireactive dendrimers showed diffraction efficiencies of 72−79% with a refractive index modulation of $1.95-2.15 \times 10^{-3}$. The volume shrinkage was also controlled to 1.56−1.41%. In addition, we demonstrated the holographic data storage including multiplexing of 10 different holograms at the same volume as well as record/retrieval of the page-wise digital data of 0.46 bits/page. We believe that the use of a nanosized photoreactive dendrimer with photopolymers will make a substantial step to the practical applications.

AUTHOR INFORMATION

Corresponding Author

*Tel.: +82-42-350-3965. Fax: +82-42-350-3910. E-mail: jungpark@kaist.ac.kr.

Notes

The authors declare no competing financial interest.

ACKNOWLEDGMENTS

This work was supported by the Brain Korea 21 Program at KAIST and also by the Korea Science and Engineering Foundation (KOSEF) Grant (WCU Program, 31-2008-000-10055-0).

REFERENCES

(1) Ozaki, M.; Kato, J.; Kawata, S. *Science* **2011**, *332*, 218−220.
(2) Juhl, A. T.; Busbee, J. D.; Koval, J. J.; Natarajan, L. V.; Tondiglia, V. P.; Vaia, R. A.; Bunning, T. J.; Braun, P. V. *ACS Nano* **2010**, *4*, 5953−5961.
(3) Moon, J. H.; Yang, S. *Chem. Rev.* **2010**, *110*, 547−574.
(4) Dhar, L.; Curtis, K.; Fäcke, T. *Nat. Photonics* **2008**, *2*, 403−405.
(5) Bruder, F.; Hagen, R.; Rölle, T.; Weiser, M.; Fäcke, T. *Angew. Chem., Int. Ed.* **2011**, *50*, 4552−4573.
(6) Dhar, L.; Schnoes, M.; Wysocki, T.; Bair, H.; Schilling, M.; Boyd, C. *Appl. Phys. Lett.* **1998**, *73*, 1337−1339.
(7) Cheben, P.; Calvo, M. L. *Appl. Phys. Lett.* **2001**, *78*, 1490−1492.
(8) Schnoes, M. G.; Dhar, L.; Schilling, M. L.; Patel, S. S.; Wiltzius, P. *Opt. Lett.* **1999**, *24*, 658−660.
(9) Carretero, L.; Murciano, A.; Blaya, S.; Ulibarrena, M.; Fimia, A. *Opt. Express* **2004**, *12*, 1780−1787.
(10) Ramos, G.; Herrero, A. A.; Belenguer, T.; Monte, F.; Levy, D. *Appl. Opt.* **2004**, *43*, 4018−4024.
(11) Waldman, D. A.; Li, H. -Y. S.; Horner, M. G. *J. Imaging Sci. Technol.* **1997**, *41*, 497−514.
(12) Waldman, D. A.; Butler, C. I.; Raguin, D. H. *Proc. SPIE* **2003**, *5216*, 10−25.
(13) Trentler, T. J.; Boyd, J. E.; Colvin, V. L. *Chem. Mater.* **2000**, *12*, 1431−1438.
(14) Jeong, Y. -C.; Lee, S.; Park, J. -K. *Opt. Express* **2007**, *15*, 1497−1504.
(15) Suzuki, N.; Tomita, Y.; Kojima, T. *Appl. Phys. Lett.* **2002**, *81*, 4121−4123.
(16) Tomita, Y.; Suzuki, N.; Chikama, K. *Opt. Lett.* **2005**, *30*, 839−841.
(17) Sanchez, C.; Escuti, M. J.; Heesch, C.; Bastiaansen, C.; Broer, D.; Loos, J.; Nussbaumer, R. *Adv. Funct. Mater.* **2005**, *15*, 1623−1629.
(18) Suzuki, N.; Tomita, Y.; Ohmori, K.; Hidaka, M.; Chikama, K. *Opt. Express* **2006**, *14*, 12712−12719.
(19) Hata, E.; Tomita, Y. *Opt. Lett.* **2010**, *35*, 396−398.
(20) Sakhno, O. V.; Goldenberg, L. M.; Stumpe, J.; Smirnova, T. N. *J. Opt. A: Pure Appl. Opt.* **2009**, *11*, 024013.
(21) Sakhno, O. V.; Goldenberg, L. M.; Stumpe, J.; Smirnova, T. N. *Nanotechnology* **2007**, *18*, 105704.
(22) Tomita, Y.; Furushima, K.; Ochi, K.; Ishizu, K.; Tanaka, A.; Ozawa, M.; Hidaka, M.; Chikama, K. *Appl. Phys. Lett.* **2006**, *88*, 071103.
(23) Khan, A.; Daugaard, A. E.; Bayles, A.; Koga, S.; Miki, Y.; Sato, K.; Enda, J.; Hvilsted, S.; Stucky, G. D.; Hawker, C. J. *Chem. Commun.* **2009**, *4*, 425−427.
(24) Kim, W. S.; Jeong, Y.-C.; Park, J.-K. *Opt. Express* **2006**, *14*, 8967−8973.
(25) Pedrón, S.; Bosch, P.; Peinado, C. J. *Photochem. Photobiol. A* **2008**, *200*, 126−140.
(26) Kim, W. S.; Jeong, Y.-C.; Park, J.-K. *Appl. Phys. Lett.* **2005**, *87*, 012106.
(27) Kim, W. S.; Jeong, Y.-C.; Park, J.-K.; Shin, C.; Kim, N. *Opt. Mater.* **2007**, *29*, 1736−1740.
(28) Franklin, J.; Wang, Z. Y. *Chem. Mater.* **2002**, *14*, 4487−4489.
(29) Kogelnik, H. *Bell Syst. Tech. J.* **1969**, *48*, 2909−2947.
(30) Jeong, Y.-C.; Jung, B.; Lee, J.; Park, J.-K. *Appl. Phys. Lett.* **2011**, *98*, 101103.
(31) Frantz, J. A.; Kostuk, R. K.; Waldman, D. A. *J. Opt. Soc. Am. A* **2004**, *21*, 378−387.